Crystallization, Heterostructure, Microstructure, and Properties of Ferroelectric Strontium Bismuth Tantalate Films Derived from Tantalum Glycolate Solutions

M. L. Calzada,*,† A. González,† J. García-López,‡ and R. Jiménez†

Inst. Ciencia de Materiales de Madrid (CSIC), Cantoblanco, 28049 Madrid, Spain, Department de Física Atómica, Nuclear y Molecular, University Sevilla, P.O. Box 1065, 41080 Sevilla, Spain, and Centro Nacional de Aceleradores (CNA), Parque Tecnológico Cartuja 93, 41092 Sevilla, Spain

Received April 4, 2003. Revised Manuscript Received September 16, 2003

Strontium bismuth tantalate (SBT) films were prepared by chemical solution deposition (CSD) onto $Pt/TiO_2/SiO_2/(100)Si$ substrates. Nominal chemical compositions of the precursor solutions of $SrBi_2Ta_2O_9$, $SrBi_{2.2}Ta_2O_9$, $Sr_{0.8}Bi_2Ta_2O_9$, and $Sr_{0.8}Bi_{2.2}Ta_2O_9$ were tested for the deposition of the films. Crystallization of the films was carried out by a two-step process (TS) or a single-step process (SS). The TS treatment consisted of thermal treatment of the films in oxygen atmosphere at 550 °C for 7200 s, with a heating rate of 8 °C/s, followed by a rapid thermal processing (RTP) in oxygen at a temperature of 650 °C for 3600 s, using a heating rate of 200 °C/s. The SS process was just the RTP treatment of the films. The X-ray diffraction (XRD) patterns of the crystalline films showed the formation of the layered perovskite together with a second phase. Analysis of the films by means of Rutherford backscattering spectroscopy (RBS) showed that this second phase was placed at the interface and it was formed by the reaction of the film and the substrate. Composition and thickness of this interface as well as profile composition of the SBT layer were also analyzed by RBS. These studies indicated that the heterostructure of the films was related with their nominal composition and with the type of thermal treatment used for their crystallization. Both parameters, composition and treatment, also determined the surface microstructures of the films. Dielectric and ferroelectric properties of the films were measured and related with their composition, heterostructure, and microstructure. The best hysteresis loops with the maximum values of remanent polarization, P_r, were obtained for the films with nominal composition of $Sr_{0.8}Bi_{2.2}Ta_2O_9$ and crystallized with the SS treatment. These films have a low fatigue up to $\sim 10^{11}$ cycles, a retention of the polarization over 10^5 seconds, and leakages of $<10^{-7}$ $\mu A/cm^2$ at 300 kV/cm.

Introduction

Nonvolatile ferroelectric random access memories (NVFeRAMs) are considered promising alternatives for nonvolatile applications.[1] For a long time, lead zirconate titanate ($PbZr_xTi_{1-x}O_3$) (PZT) thin films were considered good candidates for these devices. However, their fatigue characteristics on silicon substrates with platinum electrodes are not good enough for the requirements of NVFeRAMs.[2]

It has been observed that strontium bismuth tantalate ($SrBi_2Ta_2O_9$) (SBT) layered perovskites exhibit excellent fatigue endurance on silicon with platinum.[3] Also, on these substrates, they have better retention and lower leakage currents than PZT films.[4] The limitation to use of SBT films for memories is its crystallization temperature (usually 700−800 °C), which is too high for the integration of these films with CMOS circuits.[4] These high temperatures damage the silicon substrate. Also, reaction between the platinum electrode and the SBT layer is possible, resulting in the formation of interfaces that can be detrimental to the properties of the device and that decrease the remanent polarization, P_r, measured in the ferroelectric material. Leakages and fatigue with electric field cycling are also increased at these temperatures.

For NVFeRAMs, large P_r and low coercive field, E_c, are required in addition to the endurance property.[5] SBT is a bismuth layered perovskite formed by two pseudo-perovskite blocks, $(SrTa_2O_7)^{2-}$, between two $(Bi_2O_2)^{2+}$ layers.[5−7] Some authors have shown that the ferroelectric spontaneous polarization of this structure is affected by the nonstoichiometry of the composition.[8−10] These effects are related to the possibility of cation disorder produced by interchange of Sr and Bi positions that can lead to a variation in the ferroelectric re-

* To whom correspondence should be addressed. E-mail: lcalzada@icmm.csic.es.
† Inst. Ciencia de Materiales de Madrid (CSIC).
‡ University Sevilla and Centro Nacional de Aceleradores (CNA).

(1) Kingon, A. *Nature* **1999**, *401*, 658.
(2) Al-Shareef, H. N.; Dimos, D.; Boyle, T. J.; Warren, W. L.; Tuttle, B. A. *Appl. Phys. Lett.* **1996**, *68* (5), 690.
(3) Paz de Araujo, C. A.; Cuchiaro, J. D.; McMillan, L. D.; Scott, M. C.; Scott, J. F. *Nature* **1995**, *374*, 627.
(4) Scott, J. F.; Hartmann, A. J. *J. Phys. IV France* **1998**, *8*, 3.
(5) Shimakawa, Y.; Kubo, Y.; Tauchi, Y.; Kamiyama, T.; Asano, H.; Izumi, F. *Appl. Phys. Lett.* **2000**, *77* (17), 2749.
(6) Rae, A. D. *Acta Crystallogr.* **1992**, *B48*, 418.
(7) Shimakawa, Y.; Kubo, Y. *Appl. Phys. Lett.* **1999**, *74* (13), 1904.

10.1021/cm031065e CCC: $25.00
Published on Web 11/08/2003

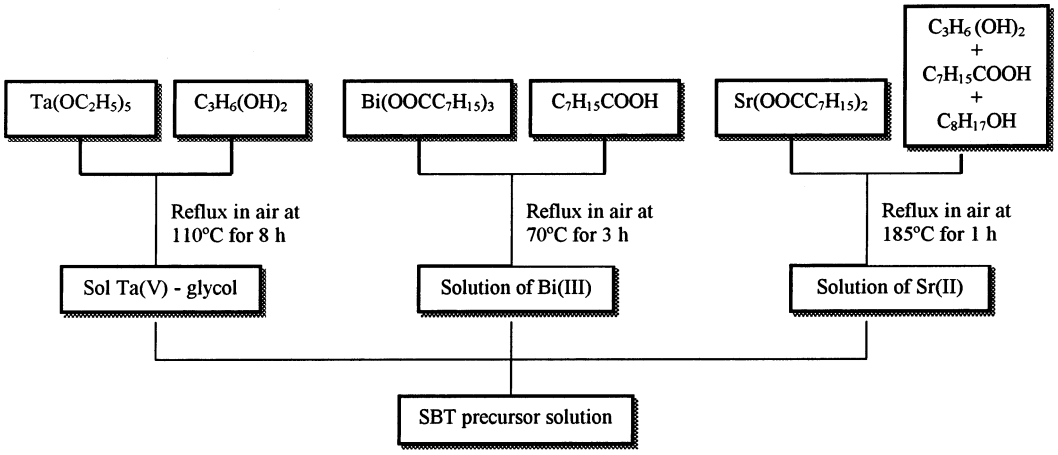

Figure 1. Scheme of preparation of the SBT precursor solutions.

sponse.[11] Deficiency and/or excess of Sr and/or Bi result in a more or less distorted structure that, in addition to a particular heterostructure and microstructure, affect the ferroelectric properties of the films, such as P_r and E_c.

This work shows the preparation by chemical solution deposition (CSD) of SBT films, using a sol−gel solution synthesized by a route previously reported.[12,13] The effectiveness of this chemical route for decreasing the formation temperature of the SBT phase down to 650 °C has been shown. Here, we study two major factors on the processing of the films: their nominal composition and the thermal treatment schedule used for their crystallization at 650 °C. Both affect the ferroelectric response of the films. Optimum processing conditions for the fabrication of films with the properties required in their use in NVFeRAMs are discussed.

Experimental Section

SBT precursor solutions with nominal compositions of $SrBi_2Ta_2O_9$, $SrBi_{2.2}Ta_2O_9$, $Sr_{0.8}Bi_2Ta_2O_9$, and $Sr_{0.8}Bi_{2.2}Ta_2O_9$ were synthesized using the tantalum glycolate route (Figure 1).[12] Advantages of this sol−gel process over others are the low toxicity and low sensitivity to moisture of the synthesized solutions, in addition to the reduction of the crystallization temperature. Stock solutions were diluted with 2-ethyl-1-hexanol, $C_8H_{17}OH$, to a concentration of 0.05 mol/L. These solutions were deposited onto $Pt/TiO_2/SiO_2/(100)Si$ substrates by spin-coating at 2000 rpm for 45 s. For the preparation of the substrates, Pt and TiO_2 layers were deposited by rf-magnetron sputtering on (100)Si substrates spontaneously oxidized in air. Pt works as bottom electrode. TiO_2 is an adhesive layer between Pt and silicon substrate and also works as a buffer layer. Wet films were dried on a hotplate at 225 °C for 900 s. Several layers of solution were successively deposited onto the substrate to increase the film thickness. Crystallization of the films was carried out in two different ways:[13] (a) a two-step process (TS) where the films were subjected to a thermal treatment in oxygen atmosphere at 550 °C for 7200 s, with a heating rate of 8 °C/s, and then a rapid thermal process (RTP) in oxygen at a temperature of 650 °C for 3600 s, using a heating rate of 200 °C/s; or (b) a single-step process (SS) where the films were directly treated by RTP in oxygen at 650 °C for 3600 s, with a heating rate of 200 °C/s.

The average thickness of the crystalline films was measured by profilometry using Taylor Hobson equipment (Talysurf 50).

Composition and heterostructure of the films were determined by means of Rutherford backscattering spectrometry (RBS). A 3 MV Tandem accelerator was used with an 8 MeV $^{14}N^{3+}$ beam. A silicon surface barrier detector with an energy resolution of 100 keV for nitrogen was set at 165° with the incident beam. Samples were tilted 6° to avoid channelling. The RBS experimental data were analyzed with the RUMP simulation code.[14] Error in the calculation of composition was ~10%. A theoretical bulk density of the SBT layer of 8.80 g/cm^3 was calculated from its molecular weight (1012 g/mol for $SrBi_2Ta_2O_9$) and crystal structure.[7] Also, for the Pt layer a theoretical bulk density of 21.45 g/cm^3 was calculated from its molecular weight of 195 g/mol and crystal structure (JCPDS-ICDD file 4-802). These densities were used for the calculation of thickness.

Crystal phases developed in the films were followed by X-ray diffraction with the conventional Bragg−Brentano geometry (XRD).

For the electrical characterization of the films, top platinum electrodes with an area of 5×10^{-6} m^2 were deposited by cold sputtering on the films' surfaces using a shadow mask. No postannealing of the electrodes was performed. Hysteresis loops were traced with a Radiant Technology Inc. testing system, RT66A model, using a triangular signal of 100 Hz of frequency and 12 V of amplitude. Fatigue and retention were recorded with the equipment joined to an external pulse generator that applied pulses of 8 V with a frequency of 500−1000 kHz. These experimental conditions used for the fatigue and retention measurements provide more than 90% of the switching without degradation of the films. Permittivity at several frequencies were measured as a function of temperature with an automatic LCR meter HP 4284 A. Permittivity data were recorded in the cooling run using a cooling rate of 2 °C/min. Leakage current densities were measured at room temperature for different positive and negative voltages, using the step voltage technique,[15] with an electrometer Keithley 6512 model and a function generator HP3325B. For all the electrical measurements, the top electrode was positively biased.

Results

Structure and Microstructure. Figure 2 shows the XRD patterns of the films crystallized with the two-step

(8) Noguchi, T.; Hase, T.; Miyasaka, Y. *Jpn. J. Appl. Phys.* **1996**, *35*, 4900.
(9) Noda, M.; Matsumuro, Y.; Sugiyama, H.; Okuyama, M. *Jpn. J. Appl. Phys.* **1999**, *38*, 2275.
(10) Noguchi, Y.; Miyayama, M.; Kudo, T. *J. Appl. Phys.* **2000**, *88* (4), 2146.
(11) Lee, J. K.; Park, B.; Hong, K. S. *J. Appl. Phys.* **2000**, *88* (5), 2825.
(12) Calzada, M. L.; Jiménez, R.; González, A.; Mendiola, J. *Chem. Mater.* **2001**, *13*, 3.
(13) Calzada, M. L.; González, A.; Jiménez, R.; Alemany, C.; Mendiola, J. *J. Eur. Ceram. Soc.* **2001**, *21*, 1517.
(14) Doolittle, L. R. *Nucl. Inst. Methods* **1985**, *B9*, 344.
(15) Waser, R.; Klee, M. *Integr. Ferroelectr.* **1992**, *2*, 23.

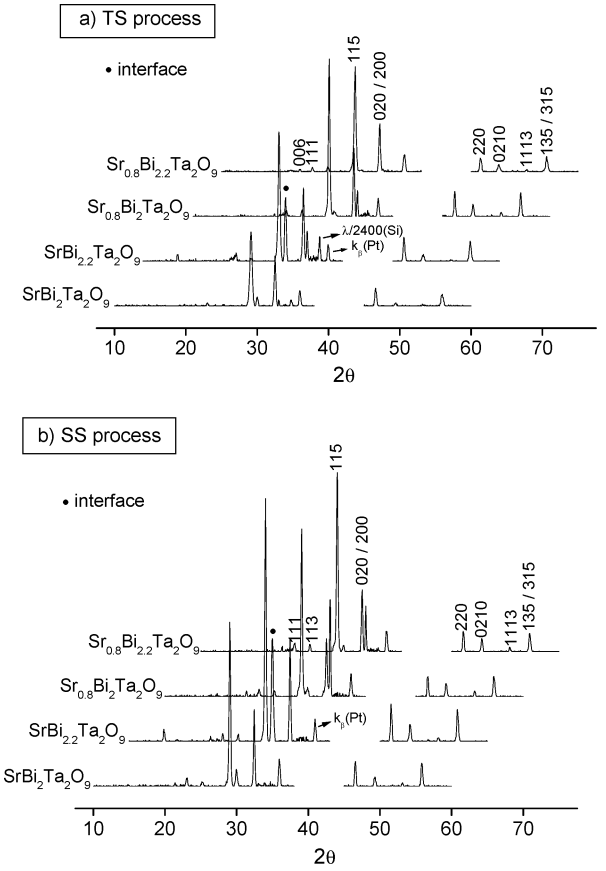

Figure 2. X-ray diffraction patterns of the films crystallized with (a) the two-step (TS) process and with (b) the single-step (SS) process. Patterns were not recorded between $2\theta \approx 37°$ and 44° to avoid the large reflection of the 111 peak of the Pt bottom electrode.

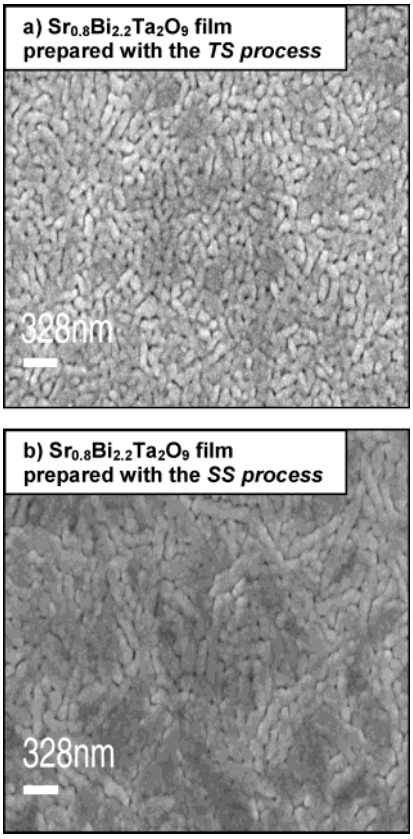

Figure 3. SEM images of the surfaces of the films crystallized with (a) the two-step (TS) process and with (b) the single-step (SS) process.

or single-step processes (TS or SS). In all the cases, formation of the layered SBT perovskite with a random orientation is observed. Besides the peaks of the SBT phase, an additional reflection appears at $2\theta \approx 30°$. The highest relative intensity of this peak (intensity of the peak compared with that of the 115 peak of the SBT) is obtained for the films with nominal composition of $SrBi_{2.2}Ta_2O_9$ crystallized with any of the treatments, TS or SS.

An example of the microstructures developed in the films crystallized with any of the two treatments are shown in Figure 3. The films with different compositions but obtained with the same thermal treatment have microstructures morphologically similar. Only outstanding differences in grain size are observed. Therefore, the images of the $Sr_{0.8}Bi_{2.2}Ta_2O_9$ films are the only ones shown here. The results of the microstructural analysis carried out on the images of the different films are summarized in Table 1, where the calculated average particle area and the axial ratio are given. The films crystallized with the TS treatment have more uniform grains with lower axial ratio than those of the films prepared with the SS treatment which results in the formation of larger nonisotropic grains (see Figure 3).[16]

Profile Composition. The RBS experimental spectra of the films and their corresponding simulations are depicted in Figure 4. Films' heterostructures deduced from these analyses are also indicated in the figure. Note that in all cases, a good fit between the experimental and the simulated curves leads to the formulation of heterostructures in which a reaction interface between the SBT film and the Pt bottom electrode is formed. The SS treatment gives rise to films with interfaces formed by Pt and Bi, whereas the interfaces of the films prepared with the TS treatment also contain O. It should be noted that the Pt bottom electrode is completely contaminated with Bi and O for the latter films, with the exception of the $Sr_{0.8}Bi_{2.2}Ta_2O_9$ film where a very thin layer of pure Pt still remains. The SS films maintain in all the cases a pure Pt layer under the Pt−Bi reaction interface. The scatter in the thickness of this layer for the different samples should be related to nonhomogeneity or roughness of the Pt. Although it is not possible to quantify the thickness of the interfaces in units of length (as we do not know the density of the compound formed at the interface), the Pt−Bi layer of the SS films seems to be much thinner than the Pt−Bi−O one formed in the TS films, as directly calculated in atoms/cm^2 from the RBS analysis (see Figure 4 and Table 1). The larger contamination of the Pt of the TS films can be observed in the RBS spectra of Figure 4 as a decrease in the intensity of the Pt signal compared with that of the SS films. We have determined this contamination degree (α) as the (Bi + O)/Pt atomic ratio obtained from the RBS data at the interface. A (Bi + O)/Pt ratio equal to zero means that the electrode is not contaminated at all, and therefore an interface is not formed. Contamination of the electrode and reaction interface increase as α increases over

(16) Ricote, J.; Calzada, M. L.; González, A.; Ocal, C. *J. Am. Ceram. Soc.*, accepted for publication.

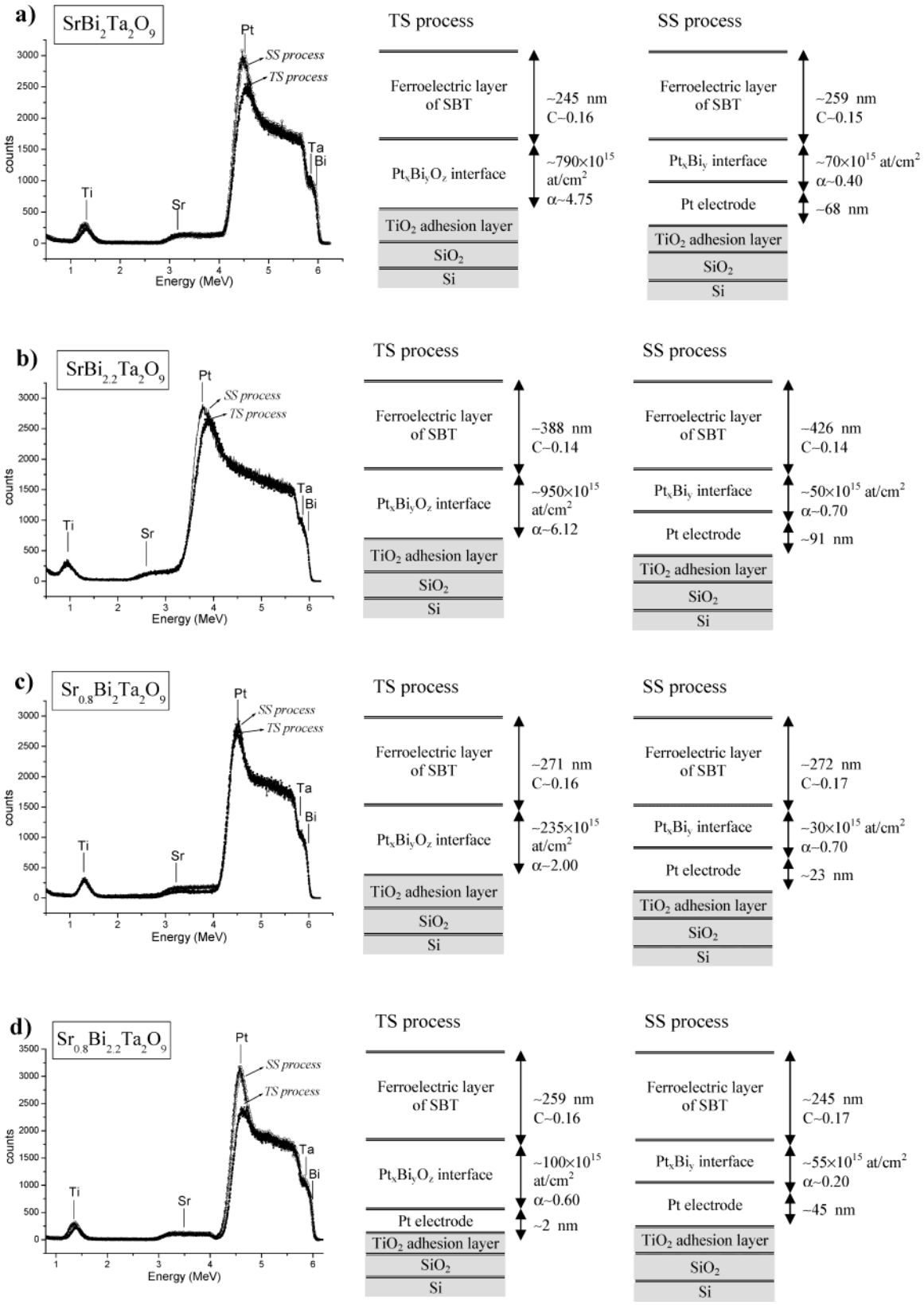

Figure 4. RBS experimental spectra and simulations together with the corresponding heterostructures of the films crystallized with the two-step (TS) process and with the single-step (SS) process, and with nominal compositions of (a) $SrBi_2Ta_2O_9$, (b) $SrBi_{2.2}Ta_2O_9$, (c) $Sr_{0.8}Bi_2Ta_2O_9$, and (d) $Sr_{0.8}Bi_{2.2}Ta_2O_9$.

zero. Values of α are indicated in the heterostructures of Figure 4.

A semiquantification of the composition of the SBT film also can be carried out considering the Bi/(Sr + Ta + O) atomic ratios (*C*) measured in this layer. The atomic ratio of the Bi cation placed in the $(Bi_2O_2)^{2+}$ layer to ions placed in the $(SrTa_2O_7)^{2-}$ perovskite is $C = 0.17$ for the stoichiometric composition ($SrBi_2Ta_2O_9$). The *C* ratios obtained here for the films are indicated in the heterostructures of Figure 4. Deviation of these values

Table 1. Parameters Measured in the Films with Different Nominal Compositions and Subjected to Different Thermal Treatments

composition	average grain size (μm^2)	axial ratio	film thickness: from profilometry (nm)	film thickness: from RBS (nm)	interface thickness from RBS ($\times 10^{15}$ atoms/cm^2)	Pt thickness from RBS (nm)	C = Bi/(Sr + Ta + O)	α = (Bi + O)/Pt	T_m (°C)	$\Delta K'$	$\Delta K'/\Delta T$ ($\times 10^{-3}$)	P_r (μC/cm^2)
Two-Step Thermal Treatment												
$SrBi_2Ta_2O_9$	0.072 ± 0.01	~2.0	~250	~245	~790		0.16 ± 0.02	4.75 ± 0.50	~194	~8	~47	~0.9
$SrBi_{2.2}Ta_2O_9$	0.039 ± 0.01	~2.2	~383	~388	~950		0.14 ± 0.02	6.12 ± 0.60	~238	~32	~150	~0.6
$Sr_{0.8}Bi_2Ta_2O_9$	0.230 ± 0.01	~2.5	~270	~271	~235		0.16 ± 0.02	2.00 ± 0.20	~287	~172	~656	~6.3
$Sr_{0.8}Bi_{2.2}Ta_2O_9$	0.120 ± 0.01	~2.6	~250	~259	~100	~2	0.16 ± 0.02	0.60 ± 0.06	~266	~103	~427	~3.3
Single-Step Thermal Treatment												
$SrBi_2Ta_2O_9$	0.170 ± 0.03	~3.3	~280	~259	~70	~68	0.15 ± 0.02	0.40 ± 0.04	~201	~39	~221	~3.6
$SrBi_{2.2}Ta_2O_9$	0.340 ± 0.02	~3.6	~450	~426	~50	~91	0.14 ± 0.02	0.70 ± 0.07	~227	~80	~396	~5.2
$Sr_{0.8}Bi_2Ta_2O_9$	0.620 ± 0.04	~3.3	~270	~272	~30	~23	0.17 ± 0.02	0.70 ± 0.07	~288	~167	~635	~8.0
$Sr_{0.8}Bi_{2.2}Ta_2O_9$	0.400 ± 0.03	~3.8	~260	~245	~55	~45	0.17 ± 0.02	0.20 ± 0.02	~267	~202	~835	~10.2

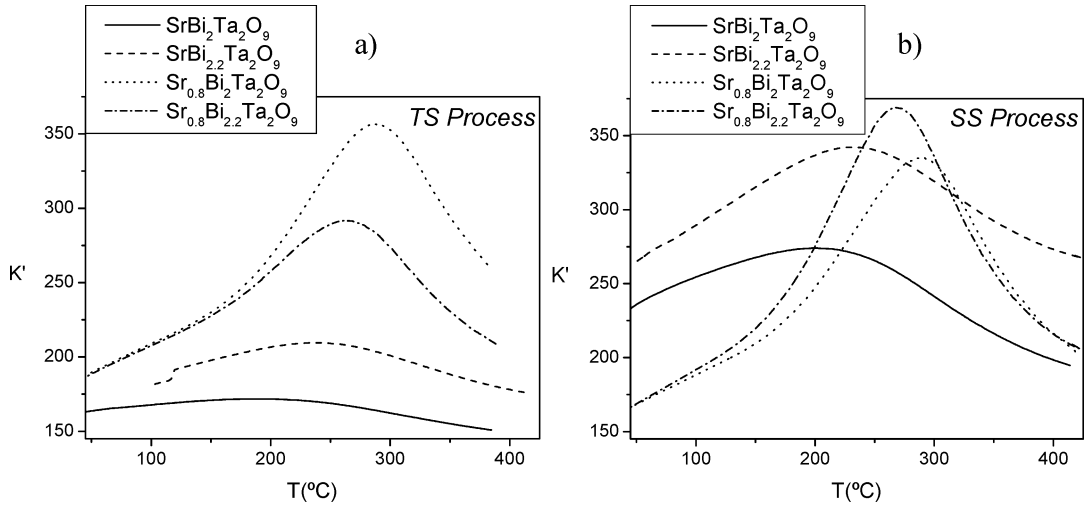

Figure 5. Variation of the dielectric constant at 10 kHz as a function of temperature for the films crystallized with (a) the two-step (TS) process and with (b) the single-step (SS) process.

from the stoichiometric one of 0.17 will be discussed in the next section. RBS results indicate that the SBT layer has a homogeneous profile composition for all the films. Thickness of the SBT layers obtained by RBS was close to that measured by profilometry. Table 1 shows the α and C values, as well as the thickness of the SBT layers, interfaces, and Pt electrodes calculated by RBS.

Dielectric and Ferroelectric Properties. Variation of the dielectric constant at 10 kHz as a function of temperature is shown in Figure 5. The temperatures at the maximum of the curve, T_m, for all the films are in Table 1 together with the differences between the dielectric constant measured at T_m and that corresponding at room temperature ($\Delta K'$ or dielectric anomaly). Dielectric anomaly is also normalized ($\Delta K'/\Delta T$) to the difference between T_m and room temperature. The T_m value gives us information about the composition of the ferroelectric layer. For a certain composition distribution, T_m corresponds to the distribution maximum. For bulk ceramics with the stoichiometric $SrBi_2Ta_2O_9$ composition, values of T_m close to 300 °C have been reported,[17] nevertheless scatter in the T_m values is found in the literature. For comparison purposes, $\Delta K'$ (or $\Delta K'/\Delta T$) can give us an idea of the ferroelectric character of the film. The stronger is the dielectric anomaly $\Delta K'$ or $\Delta K'/\Delta T$, the larger is the amount of ferroelectric phase in the film and the smaller the content of second phases (porosity, grain boundaries, second nonferroelectric phases dispersed in the material, or in series, etc.). For both types of treatments, the T_m value closest to 300 °C is always obtained in the $Sr_{0.8}Bi_2Ta_2O_9$ films. Among the TS crystallized films, the film of this composition has also the largest $\Delta K'$. However, for the SS crystallized films, the $Sr_{0.8}Bi_{2.2}Ta_2O_9$ film is that with the largest $\Delta K'$. Those films without Sr defect have low T_m and small $\Delta K'$. Comparing the films with the same nominal composition but subjected to different thermal treatment, differences in T_m are very small. This shows that the films have close compositions. However, dielectric anomalies $\Delta K'$ are quite different. $\Delta K'$ is larger in the SS films (except for the $Sr_{0.8}Bi_2Ta_2O_9$ films), which is an indication of a larger content of ferroelectric phase in the SS films than in the TS films.

Figures 6 and 7 show the hysteresis loops of the films and their corresponding loop derivatives, respectively. P_r values obtained from these loops are in Table 1. P_r and the derivative measured at the coercive field, E_c, are always smaller for the films crystallized with the TS treatment than for those prepared with the SS treatment. The largest P_r value is that of the film with nominal composition of $Sr_{0.8}Bi_{2.2}Ta_2O_9$ crystallized with the SS process.

(17) Komura, K.; Nagata, H.; Takenaka, T. *Ferroelectrics* **1998**, *218*, 233.

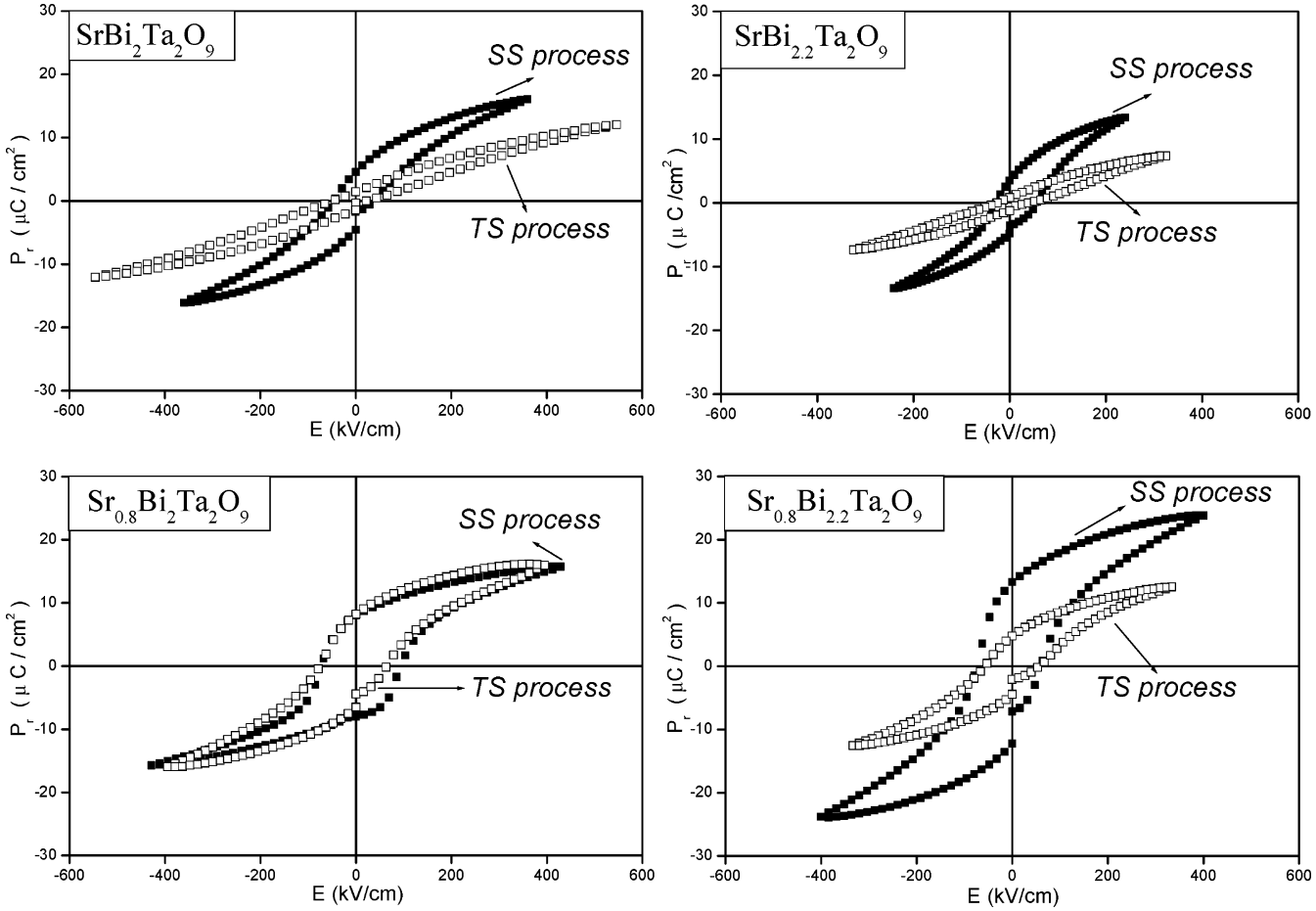

Figure 6. Ferroelectric hysteresis loops of the films with different nominal compositions ($SrBi_2Ta_2O_9$, $SrBi_{2.2}Ta_2O_9$, $Sr_{0.8}Bi_2Ta_2O_9$, and $Sr_{0.8}Bi_{2.2}Ta_2O_9$) and crystallized with different thermal treatments (two-step (TS) or single-step (SS) processes).

Discussion

Solution Composition and Thermal Treatment of Crystallization. The effect of composition of the precursor solutions on the formation of SBT films prepared by CSD has been previously studied by other authors.[18,19] Compositions with small deviations of strontium and/or bismuth from the stoichiometric one ($SrBi_2Ta_2O_9$) can give rise to the formation of second phases. SBT precursor solutions containing stoichiometric Bi and a large Sr defect can lead to SBT films with bismuth tantalate, $BiTaO_4$, as second phase.[8] In contrast, films derived from solutions with a large Bi excess and stoichiometric Sr usually contain a segregated Bi_2O_3 phase in the bulk film, metallic Bi on the film surface,[4] Bi−Pt interfaces,[20] or segregated Bi at the grain boundaries. Also, a cation disorder has been recently reported as possible in the SBT structure.[11] Sr can occupy Bi positions at the $(Bi_2O_2)^{2+}$ layers in a lower extension than the Bi can occupy Sr sites at the perovskite units. As commented before, these compositional and structural factors affect the ferroelectric response of the films. Thus, an increase in the P_r values has been reported for films containing at the same time Bi excess and Sr defect.[21]

About the type of thermal treatment, studies carried out by other authors have shown how the use of short-time thermal processes (RTP treatments) and low crystallization temperatures (650 °C) can lead to the direct crystallization of the ferroelectric phase and to the decrease of the reaction interface between the ferroelectric layer and the electrode.[22] Also, the thermal processing affects the film microstructure. Therefore, selection of appropriate treatments of crystallization results in films with better ferroelectric responses.[23,24]

Small amounts of fluorite second phase have been detected in some SBT films crystallized at temperatures lower than 700 °C.[25] This fluorite has a composition close to that of the layered perovskite, and it is a nanocrystalline phase not easily observed by XRD. Here, an extra peak is clearly detected in the X-ray patterns of Figure 2 at $2\theta \approx 30°$, that cannot be assigned to the fluorite. Neither morphologically differentiated second phases from the SBT grains are distinguished in the films microstructures (Figure 3). Previous TEM work preformed by the authors[25] demonstrated the existence

(18) Koiwa, I.; Kanehara, T.; Mita, J. *Jpn. J. Appl. Phys.* **1996**, *36*, 1597.
(19) Koiwa, I.; Okada, Y.; Mita, J.; Hashimoto, A.; Sawada, Y. *Jpn. J. Appl. Phys.* **1996**, *36*, 5904.
(20) Li, A.; Wu, D.; Ling, H.; Yu, T.; Wand, M.; Yin, X.; Liu, Z.; Ming, N. *Thin Solid Films* **2000**, *375*, 215.
(21) Tanaka, M.; Hironaka, K.; Onodera, A. *Jpn. J. Appl. Phys.* **2000**, *39*, 5472.
(22) Uchiyama, K.; Arita, K.; Shimada, Y.; Hayashi, S.; Fujii, E.; Otsuki, T.; Solayappan, N.; Joshi, J.; Paz de Araujo, C. A. *Integr. Ferroelectr.* **2000**, *30*, 103.
(23) Kim, S. H.; Kim, C. E.; Oh, Y. J. *J. Mater. Sci.* **1995**, *30*, 5639.
(24) Moert, M.; Mikolajick, T.; Shindler, G.; Magel, N.; Hartner, W.; Dehm, C.; Kohlstedt, H.; Waser, R. *Appl. Phys. Lett.* **2002**, *81* (23), 4410.
(25) Ricote, J.; Jiménez, R.; Calzada, M. L.; González, A.; Mendiola, J. *Ferroelectrics* **2003**, *271*, 143.

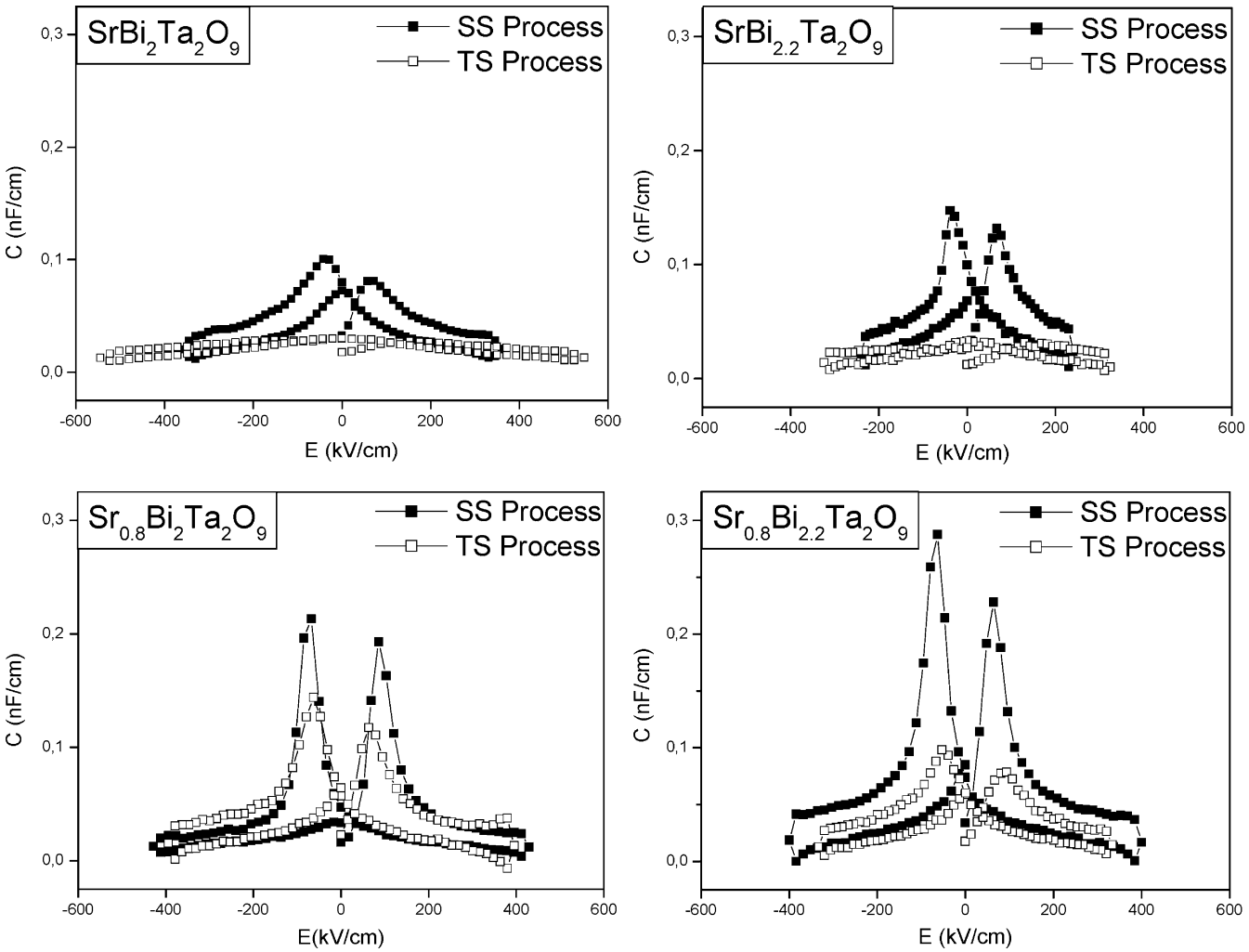

Figure 7. Ferroelectric hysteresis loop derivatives of the films with different nominal compositions ($SrBi_2Ta_2O_9$, $SrBi_{2.2}Ta_2O_9$, $Sr_{0.8}Bi_2Ta_2O_9$, and $Sr_{0.8}Bi_{2.2}Ta_2O_9$) and crystallized with different thermal treatments (two-step (TS) or single-step (SS) processes).

of small amounts of fluorite dispersed in the bulk of the film. The thicker the film was, the lower the amount of fluorite. The fluorite content was very low for films with thickness close to that of the films of this work, and thus, its effect on the ferroelectric properties was negligible.

Formation of Pt−Bi Based Interfaces. The reflection at $2\theta \approx 30°$ has been assigned by other authors to a Pt−Bi compound (Pt_xBi_y),[26] a bismuth tantalate ($BiTaO_4$),[8] or a bismuth titanate ($Bi_4Ti_3O_{12}$).[27] $BiTaO_4$ has been found in SBT films with large Sr deficiencies (>30 mol %), whereas $Bi_4Ti_3O_{12}$ appears in films deposited onto silicon substrates with Ti layers (Pt/Ti/SiO_2/(100)-Si or Ti/Pt/Ti/SiO_2/(100)Si).[27,28] Formation of $Bi_4Ti_3O_{12}$ is not possible in the films of this work because the substrate here used is Pt/TiO_2/SiO_2/(100)Si,[28] neither is crystallization of $BiTaO_4$ easy in these films with Sr deficiencies smaller than 30 mol %. Therefore, this peak should be due to the formation of a Pt−Bi based compound, as confirmed from the RBS results of Figure 4.

Study of the films' heterostructures by RBS (Figure 4) indicates that a substrate−film interface is formed in all the films. This interface is due to the reaction of Bi and Pt. But in the case of the TS treatment, where the reaction time between substrate and film is larger (a treatment at 550 °C/2 h previous to the RTP crystallization at 650 °C/1 h), the interface also contains O and affects the whole Pt electrode thickness. This is in agreement with Y. Shimakawa et al.[29] who reported how the Bi−Pt alloy rapidly takes up oxygen in an oxidizing environment. The Bi−Pt oxide is formed at low temperatures of ∼550 °C. At temperatures over 700 °C, the oxide releases oxygen and changes to Pt metal. Among the films obtained with the TS treatment, the $SrBi_{2.2}Ta_2O_9$ film has the highest contamination degree of the Pt of the interface (see Figure 4 and Table 1). In this film, migration of the Bi excess toward the Pt electrode should be easy. However, in the films with nominal compositions containing Sr defect, a decrease in the thickness and contamination of the interface is observed. Here, Bi can occupy the Sr vacancies in the SBT structure where it is trapped, thus reducing its diffusion to the substrate. For the films processed with the SS treatment, the interfaces are less contaminated and are

(26) Bartz, R.; Amrhein, F.; Shin, Y. W.; Dey, S. K. *Integr. Ferroelectr.* **1998**, *22*, 65.
(27) Seong, N. J.; Yand, C. H.; Shin, W. C.; Yoon, S. G. *Appl. Phys. Lett.* **1998**, *72* (11), 1374.
(28) González, A. PhD Thesis, University Autónoma de Madrid (Spain), January, 2003.
(29) Shimakawa, Y.; Kubo, Y. *Mater. Res. Soc. Symp. Proc.* **2000**, *596*, 131.

oxygen free. Again, the $Sr_{0.8}Bi_{2.2}Ta_2O_9$ film has the less contaminated interface with the smallest α value (see Figure 4 and Table 1).

Composition of the SBT Layer. Concerning the composition of the SBT layer, the results show that the films with the same nominal composition but obtained with different processes, TS or SS, have close C values. This indicates a similar average composition. Composition can also be discussed as a function of the variation of T_m. Film stresses shift the T_m values.[30,31] Therefore, we must assume that stresses are similar in all of the films. This assumption is supported by the fact that the films were deposited from solutions with the same concentration, they have similar thickness, and the type of thermal treatment seems to have no strong effect on them (note that TS and SS films with the same nominal composition have very close values of T_m, see Table 1). Taking into account these considerations, the T_m values could be related with the composition of the SBT layer determined by RBS (C = Bi/(Sr + Ta + O)). These T_m values confirm that the maximums in the composition distribution are very similar for the TS and SS films with the same nominal composition. However, appreciable differences are measured in their dielectric anomalies, $\Delta K'$. $\Delta K'$ and also $\Delta K'/\Delta T$ are always larger in the SS films than in the TS ones, indicating that the content of ferroelectric phase is larger in the former than in the latter. Looking at the microstructures of both types of films (see Table 1), it can be noted that the TS films have smaller grain size than the SS films. This means more grain boundaries. Grain boundaries usually contain nonferroelectric segregated phases, mainly formed, in this particular case, by the migration of Bi from the grain to the boundary. This would justify the close average composition of the TS and SS films derived from solutions with the same nominal composition, but their different ferroelectric response. Larger P_r values are measured for the SS films than for the TS films.

Comparing films with different nominal compositions, it can be observed in Table 1 how T_m increases as C increases. The maximum T_m values are obtained for those films with $C = 0.17 \pm 0.02$ or 0.16 ± 0.02 (~288 °C for the $Sr_{0.8}Bi_2Ta_2O_9$ films and ~267 °C for the $Sr_{0.8}Bi_{2.2}Ta_2O_9$ films), whereas the minimum T_m values are those of the films with stoichiometric Sr ($SrBi_2Ta_2O_9$ and $SrBi_{2.2}Ta_2O_9$ films). Similar evolution of T_m with film composition has been reported by Takemura et al.[32] They also found how Sr deficient films exhibit stronger dielectric anomalies $\Delta K'$ than the others. Here, the $Sr_{0.8}Bi_{2.2}Ta_2O_9$ film processed with the SS treatment has the largest $\Delta K' = 202$, despite the fact that its T_m is slightly lower than that of the SS processed $Sr_{0.8}Bi_2Ta_2O_9$ film. This is also in accordance with Takemura et al.[32]

Ferroelectric Properties related to Composition, Heterostructure, and Microstructure of the Films. Film and interface compositions have a large effect on the ferroelectric response of SBT films.[10,13,33] In this work, the P_r values obtained from the hysteresis loops for the TS films are lower than those of the films prepared with the SS treatment (Figure 6). Also, the loop derivatives are larger in the SS treated films (Figure 7). Reduction of P_r and its derivative is related to the presence of secondary nonferroelectric phases, with this being stronger for in-series distributions.[34] The films with the nominal compositions of $SrBi_2Ta_2O_9$, $SrBi_{2.2}Ta_2O_9$, and $Sr_{0.8}Bi_{2.2}Ta_2O_9$ show a strong change in their ferroelectric properties when crystallized with the TS treatment or with the SS treatment. This can be directly related to the different characteristics of their interfaces and SBT layers (see Figure 4 and Table 1). But, note the properties of the $Sr_{0.8}Bi_2Ta_2O_9$ films where similar hysteresis loops were obtained for both types of thermal treatments. In this case, the films present microstructural parameters that can be responsible for this behavior. These films have the largest grain size for both TS and SS treatments. This size is of the same order or even larger than the film thickness. Thus, not many grain boundaries, which would decrease the ferroelectric response, are expected through the film thickness, where the electrical measurements are carried out (electric field is applied in the perpendicular direction to the surface, from the top to the bottom electrode). In contrast, the $SrBi_{2.2}Ta_2O_9$ TS films have the worst ferroelectric properties, probably due to, among others factors here discussed, their large thickness compared with their small grain size (see Figure 6 and Table 1). On the other hand, it has been previously shown by the authors[16] that the grain size of TS films does not change with a re-crystallization step at high temperatures (700 °C). This is probably related to the formation of defective grain boundaries in these films which hinder grain sintering.

Use of the Films in Nonvolatile Memories. For all the films studied here, the $Sr_{0.8}Bi_{2.2}Ta_2O_9$ film obtained with the SS process is that with the largest P_r value. This is in accordance with its small interface and an appropriate composition of the SBT layer joined to few grain boundaries. In this film, the Bi excess of the nominal composition can migrate toward the substrate or to the grain boundary, but also can occupy the Sr vacancies. The results indicate that the dominant process is the occupation of the Sr vacancies by the Bi excess, more than the diffusion of the Bi toward the Pt bottom electrode or to the grain boundary. Other authors[22] have shown that SBT compositions with Bi in Sr positions produce a structural distortion of the pseudo-perovskite that results in maximum values of spontaneous and remanent polarizations, P_s and P_r. But, this also decreases the reaction interface between Pt and Bi. Consequently, the Bi defect in the SBT layer is low, improving stoichiometry and crystallinity of the ferroelectric phase which results in appropriate dielectric and ferroelectric properties (T_m, $\Delta K'$, and P_r). It should be noted that some authors[20,26] emphasized the role of the $PtBi_2$ interface on the ferroelectric properties degradation. Our results show that the interface contamination produces a detrimental effect on the properties, but that the film microstructure (grain size and grain bound-

(30) Spierings, G. A. C. M.; Dormans, G. J. M.; Moors, W. G. J.; Ulenaers, M. J. E.; Larsen, P. K. *J. Appl. Phys.* **1995**, *78*, 1926.
(31) Mendiola, J.; Calzada, M. L.; Ramos, P.; Martín, M. J.; Agulló-Rueda, F. *Thin Solid Films* **1998**, *315*, 195.
(32) Takemura, K.; Noguchi, T.; Hase, T.; Miyasaka, Y. *Appl. Phys. Lett.* **1998**, *73* (12), 1649.
(33) Cheong, C.; Kim, J. S. *Integr. Ferroelectr.* **1998**, *21*, 229.
(34) Jiménez, R.; Alemany, C.; Calzada, M. L.; González, A.; Ricote, J.; Mendiola, J. *Appl. Phys. A.* **2002**, *75*, 607.

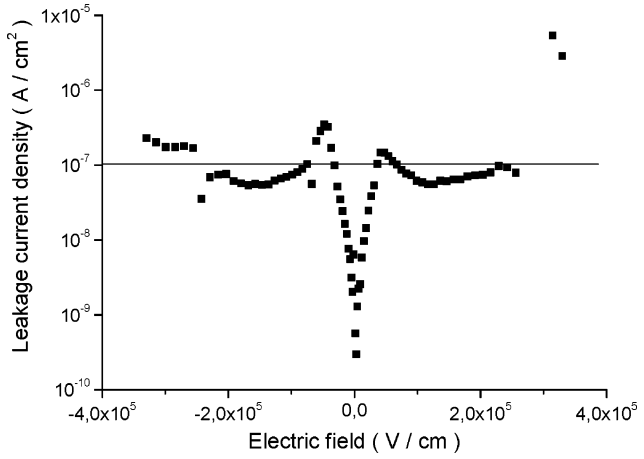

Figure 8. Leakage current densities measured at room temperature for the $Sr_{0.8}Bi_{2.2}Ta_2O_9$ film crystallized with the SS process.

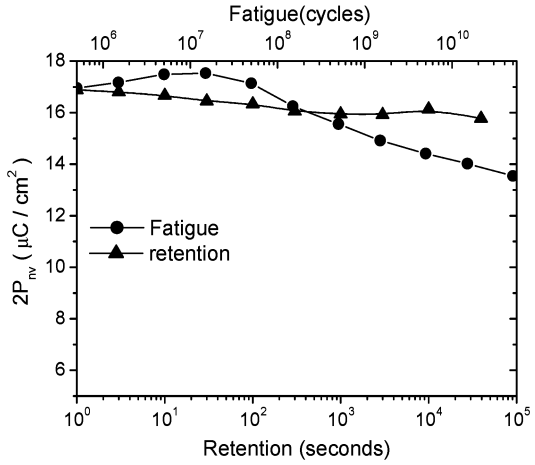

Figure 9. Fatigue and retention of the $Sr_{0.8}Bi_{2.2}Ta_2O_9$ film crystallized with the SS process.

aries) also plays an important role in the final ferroelectric properties of the films.

Taking into account the former discussion, evaluation of the films for their use in NVFeRAMs was carried out only for the $Sr_{0.8}Bi_{2.2}Ta_2O_9$ films crystallized with the SS treatment. Leakages, fatigue, and retention were measured in this film. These results are shown in the Figures 8 and 9.

Leakages of these films are shown in Figure 8. A value of $<10^{-7}$ μA/cm^2 at 300 kV/cm is obtained. The evolution of the nonvolatile polarization P_{nv}[35] in this film (Figure 6) with the number of cycles (Figure 9) shows a low fatigue up to 10^{11} cycles. This film also has a small reduction (10%) of P_{nv} after 10^5 seconds (retention, Figure 9). P_r values, leakages, fatigue, and retention obtained in this SBT film are comparable to those reported by other authors[3,36−40] and they show the interest of these films for their use in NVFeRAMs.[41−43]

Conclusions

Thermal Treatment of Crystallization. (a) Thermal treatment of crystallization of chemical-solution-deposited strontium bismuth tantalate (SBT) films produces reaction between the SBT layer and the substrate ($Pt/TiO_2/(100)SiO_2$), giving rise to film−substrate interfaces. (b) Formation of the interfaces is due to the migration of the Bi from the SBT layer toward the substrate and to the reaction of this Bi with the Pt bottom electrode. (c) Short thermal treatments (single-step treatment, SS) minimize diffusion phenomena, leading to films with thinner and less contaminated interfaces, as compared with the interfaces of the films crystallized with long thermal treatments (two-step treatment, TS). (d) The SS treatment produces SBT films formed by anisotropic grains with larger grain sizes than those of the isotropic grains formed in the films crystallized with the TS treatment. (e) Larger dielectric anomalies ($\Delta K'$ and $\Delta K'/\Delta T$) and remanent polarizations (P_r) are always measured in the films crystallized with the SS treatment than in those prepared with the TS treatment. This indicates that the content of ferroelectric phase is larger in the SS films than in TS films.

Nominal Composition. (a) Films derived from solutions with the same nominal composition have, after crystallization, close Bi/(Sr + Ta + O) ratios independently of the type of thermal treatment (SS or TS) and close T_m values (temperature at the maximum of the dielectric constant vs temperature). This indicates a similar average composition. (b) Films prepared from solutions with Bi excess and Sr defect develop thin and low contaminated interfaces. Here, the Bi excess occupies the Sr vacancies instead of migrating toward the substrate. (c) The former films after crystallization have a homogeneous profile composition with a Bi/(Sr + Ta + O) atomic ratio close to the stoichiometric one. (d) Maximum T_m values are obtained for those films with Sr defect. These films also have the maximum dielectric anomalies ($\Delta K'$ and $\Delta K'/\Delta T$) which is an indication of a clear ferroelectric character.

Nonvolatile Applications. The film deposited from solutions with Bi excess and Sr defect (nominal composition of $Sr_{0.8}Bi_{2.2}Ta_2O_9$), and crystallized with the short thermal treatment (SS) exhibits the largest dielectric anomaly ($\Delta K'$) and the maximum value of remanent polarization ($P_r \approx 10.2$ μC/cm^2). This film also has low leakages of $<10^{-7}$ μA/cm^2 at 300 kV/cm, low fatigue up to 10^{11} cycles, and 90% retention at 10^5 s.

Acknowledgment. This work has been supported by the Spanish project MAT2000-1925-CE. J. García-López and R. Jiménez acknowledge the "Ramon y Cajal" program of the Spanish MCyT for financial support.

CM031065E

(35) Dat, R.; Litchenwalner, D. J.; Auciello, O.; Kingon, A. I. *Integr. Ferroelectr.* **1994**, *5*, 275.
(36) Lakeman, C. D. E.; Boyle, T. J. *Mater. Res. Soc. Symp. Proc.* **1999**, *541*, 259.
(37) Lee, K. S.; Sohn, D. S.; Hong, S. H.; Lee, W. I.; Kim, Y.; Chae, H. K.; Chung, I. *Thin Solid Films* **2001**, *394*, 142.
(38) Mihara, T.; Yoshimori, H.; Watanabe, H.; Paz de Araujo, C. A. *Jpn. J. Appl. Phys.* **1995**, *34*, 5233.
(39) Celinska, J.; Hoshi, V.; Norayan, S.; McMillan, L. D.; Paz de Araujo, C. A. *Integr. Ferroelectr.* **2000**, *30*, 103.
(40) Ling, H.; Li, A.; Wu, D.; Yu, T.; Zhu, X.; Yin, X.; Wand, M.; Lir, Z.; Ming, M. *Integr. Ferroelectr.* **2001**, *33*, 253.
(41) Auciello, O.; Scott, J. F.; Ramesh, R. *Phys. Today* **1998**, *7*, 22.
(42) Scott, J. F. *Ferroelectr. Rev.* **1998**, *1*, 1.
(43) Scott, J. F. *Ferroelectric Memories*; Springer Series in Advanced Microelectronics; Springer-Verlag: Berlin, 2000.